IMPORTANT NOTICE: The current official version of this document is available via the Sandia National Laboratories WIPP Online Documents web site. A printed copy of this document may not be the version currently in effect.

SANDIA NATIONAL LABORATORIES
WASTE ISOLATION PILOT PLANT

AP-178
Revision 0

Analysis Plan for Reconsideration of the WIPP Geomechanical Model for Room Closure

Task 4.4.2.4.1

Effective Date: September 21, 2017

Authored by:	Dwayne Kicker	*Original signed by Dwayne Kicker*	*9/21/2017*
	Print Name	Signature	Date
Authored by:	Benjamin Reedlunn	*Original signed by Dwayne Kicker for*	*9/21/2017*
	Print Name	Signature	Date
Authored by:	Courtney Herrick	*Original signed by Dwayne Kicker for*	*9/21/2017*
	Print Name	Signature	Date
Reviewed by:	Ramesh Sarathi	*Original signed by Ramesh Sarathi*	*9/21/2017*
	Print Name Technical Reviewer	Signature	Date
Reviewed by:	Shelly Nielsen	*Original signed by Shelly R. Nielsen*	*9-21-17*
	Print Name Quality Assurance Reviewer	Signature	Date
Approved by:	Christi Leigh	*Original signed by Christi Leigh*	*9-21-17*
	Print Name Department Manager	Signature	Date

© 2017 NTES of Sandia, LLC.

Table of Contents

1 Introduction and Objectives 3
2 Background 4
3 Approach 12
3.1 Assessment of Model Predictions of Room Closure 13
3.2 Assessment of Laboratory Test Results 20
3.3 Numerical Modeling Techniques 21
3.4 Development of an Updated WIPP Conceptual Geomechanical Model for Room Closure 21
4 Reports and Documentation 22
5 Tasks 23
6 Software 23
7 Special Considerations 23
8 Applicable Procedures 23
9 References 24

1 Introduction and Objectives

The Waste Isolation Pilot Plant (WIPP), located in southeastern New Mexico, has been developed by the U.S. Department of Energy (DOE) for the geologic (deep underground) disposal of transuranic (TRU) waste. Containment of TRU waste at WIPP is regulated by the U.S. Environmental Protection Agency (EPA) according to the regulations set forth in Title 40 of the Code of Federal Regulations (CFR), Part 191. DOE demonstrates compliance with the containment requirements according to the Certification Criteria in Title 40 CFR Part 194 by means of performance assessment (PA) calculations performed by Sandia National Laboratories (SNL). WIPP PA calculations estimate the probability and consequence of potential radionuclide releases from the repository to the accessible environment for a regulatory period of 10,000 years after facility closure. The models used in PA are maintained and updated with new information as part of an ongoing process. Improved information regarding important WIPP features, events, and processes typically results in refinements and modifications to PA models and the parameters used in them. Planned changes to the repository and/or the components therein also typically result in updates to WIPP PA models. WIPP PA models are used to support the repository recertification process that occurs at five-year intervals following the receipt of the first waste shipment at the site in 1999.

The current conceptual model for the geomechanical closure of excavated rooms at WIPP considers creep closure – the gradual, continuous movement of salt from the formation into the void space of the rooms. It does not address discrete events like rock fall and floor heave. Recent experience at WIPP has highlighted the occurrence of discrete closure mechanisms. The February 2014 radiological release event at WIPP halted waste emplacement activities at the facility for approximately three years. While clean-up of the contaminated areas was underway, underground access was limited, and routine ground control maintenance activities were not possible. Ground conditions deteriorated significantly during this time, resulting in the following discrete closure phenomena:

- Three roof fall events (Panel 4 access drift S-3650; Panel 3 access drift S-2750; and Panel 7, Room 4)
- Severe roof sagging (Main access drift E-300; Main access drift E-140 south of S-1600)
- Severe floor heave (Main access drift E-300)
- Pervasive roof tension fracturing resulting in detached rock slabs (Main access drift E-300 between S-1950 and S-3080)
- Extensive rib fracturing (Panel 7 access drift S-2180; Panel 8, Room 1; Main access drift W-170 south of S-1600).

As a result, to protect workers, DOE decided to restrict access to the south end of the mine, and is proposing to abandon a set of open drifts (i.e., Panel 9) that were originally planned to hold waste.

Currently, the WIPP PA models for room closure cannot simulate discrete events like rock fall and floor heave. The proposed layout change of the WIPP repository – an abandoned panel with no

waste emplaced – coupled with recent observations of roof, rib, and floor instability and failure has led to a need to reconsider the WIPP geomechanical conceptual model. The objectives of the analyses described in this analysis plan are to (1) conceptualize room closure behavior with a focus on discrete mechanisms, and (2) develop the approach used to assess the impact of an open, unfilled panel on the long-term performance of the repository. The analyses performed are compliance decision analyses.

2 Background

Thermo-mechanical simulations are an essential component of salt repository science. Simulations play an important role in predicting the waste isolation process. Simulations also provide short-term predictions that are valuable to the operation and design of salt repositories. For example, operations personnel need to know how long they can operate in an area before it becomes unsafe. Simulations that include the disturbed rock zone can help predict when a slab of salt might detach from the roof and fall to the floor. As another example, repository operators may wish to backfill a large area with crushed salt or seal off a section of the repository. Many seal designs rely on drift closure to compress the seal, so simulations can help predict the seal maturation time. As one further example, engineers must consider operational efficiency, worker safety, environmental impact, costs, and many other factors when they lay out a repository design. Simulations of the underground evolution can be quite helpful to select between various design concepts. For these reasons and others, it is important to invest in geomechanical modeling tools.

Room D was an in-situ, isothermal, underground experiment conducted at WIPP between 1984 and 1991. The room was carefully instrumented to measure the horizontal and vertical closure immediately upon excavation and for several years thereafter. Early finite element simulations of salt creep around Room D under-predicted the vertical closure by 4.5 times, causing investigators to explore a series of changes to the way Room D was modeled. Discrepancies between simulations and measurements were resolved through a series of adjustments to model parameters, which were openly acknowledged in published reports.

Interest in Room D has been rekindled recently by the U.S./German Joint Project III and Project WEIMOS, which seek to improve the predictions of rock salt constitutive models. Joint Project participants calibrate their models solely against laboratory tests and benchmark the models against underground experiments, such as Room D at the WIPP.

Fracturing of the rock occurs around all sides of underground openings at WIPP. The fracturing requires a different modeling approach to simulate behavior of the underground. The material cannot be treated as a continuum without modification to account for the fracture surfaces.

The fracturing that occurs around every underground opening is an integral part of the disturbed rock zone (DRZ). Evidence for ubiquitous fracturing includes the formation of thick rock slabs in the roof delineated by low-angle fractures, tension cracks in the slabs at locations of extensive curvature, floor heave, spalling of the ribs and corners, separation along anhydrite stringers or clay seams, and multiple extensile and shear fracture sets in the ribs and roof. Nuclear Waste Partnership (NWP), who is the Management and Operating Contractor for DOE's Carlsbad Field

Office (CBFO), is responsible for assessing the operational stability and performance of the WIPP underground facility. NWP distinguishes rock failure modes around rooms between those types that generally occur in the lower horizon from those in the upper horizon (Figure 1). Most underground excavations at WIPP are located in the lower horizon where a clay layer known as "Clay G" is located about 8 feet above the roof line (Figure 1A). Some portions of the WIPP facility, including Panels 3, 4, 5, and 6, have been excavated slightly higher in the salt sequence so that Clay G forms the immediate roof line (Figure 1B). The primary difference between the failure modes of salt in the two horizons is what occurs in the roof of the openings.

As depicted in Figure 1A, a rock slab delineated by low-angle fractures occurs in the lower horizon. The low-angle fractures appear to be the result of the coalescence of *en echelon* fractures that intersect the corners of the roof and ribs. The low-angle fractures may grow and intersect each other in approximately the center of the opening, forming a triangular rock block as drawn in Figure 1A. It is equally possible that the low-angle fractures intersect a clay seam/anhydrite layer. Generally, the clay seam/anhydrite layer separates because the layer is very weak in tension and is not able to resist the pull of gravity on the rock block. If this is the case, the rock block becomes trapezoidal in shape. In both cases it can be assumed that the slabs are completely detached and are held up only by rock bolts, chain-link mesh, and steel slats. Cross-sectional shapes of the roof fall in SPDV Room 1 show both triangular and trapezoidal shaped blocks (Figure 2). Figure 3 shows some photographs in the WIPP underground of salt rock slabs in the roof delineated by low-angle fractures. Evident in all slides is separation along the clay seam/anhydrite layer above the opening. It should also be noted that as the rock slab deforms, the lower surface becomes increasingly curved. Eventually the curvature becomes too much for the salt to withstand and tensile fractures form. The most pronounced example of tensile fracturing in highly-curved, detached slabs can be seen in the E-140 drift (Figure 4). In Figure 4, the chain-link mesh is stretched tight, the steel support slats have been pulled apart by tensile forces, and there is a visible tensile fracture approximately in the middle of the bow. In the upper picture the salt slabs have rotated downward and form an angle of approximately 45° with the rib on the right side of the picture. Bowing of the slabs also produces shear along the clay seams which is noted in the vertical observation boreholes.

Floor heave is also common throughout the repository. An extreme example of floor heave occurred in the lower horizon, Panel 7 (Figure 5). In this instance, several slabs of salt approximately equal in thickness buckled as they were compressed from the ribs due to salt creep and lateral deformation due to pillar shortening. Not only did the slabs bow in the middle, but they also rotated upwards towards the center of the opening. Large gaps formed between the slabs. In Figure 5, the floor is being excavated down to Marker Bed 139.

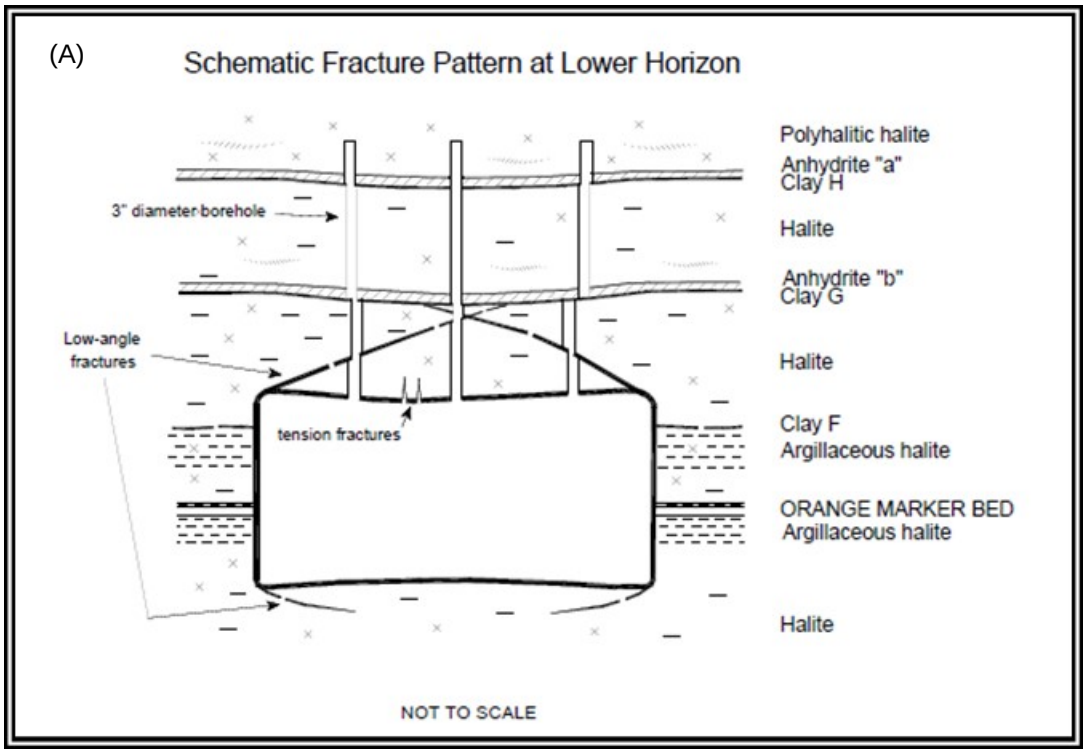

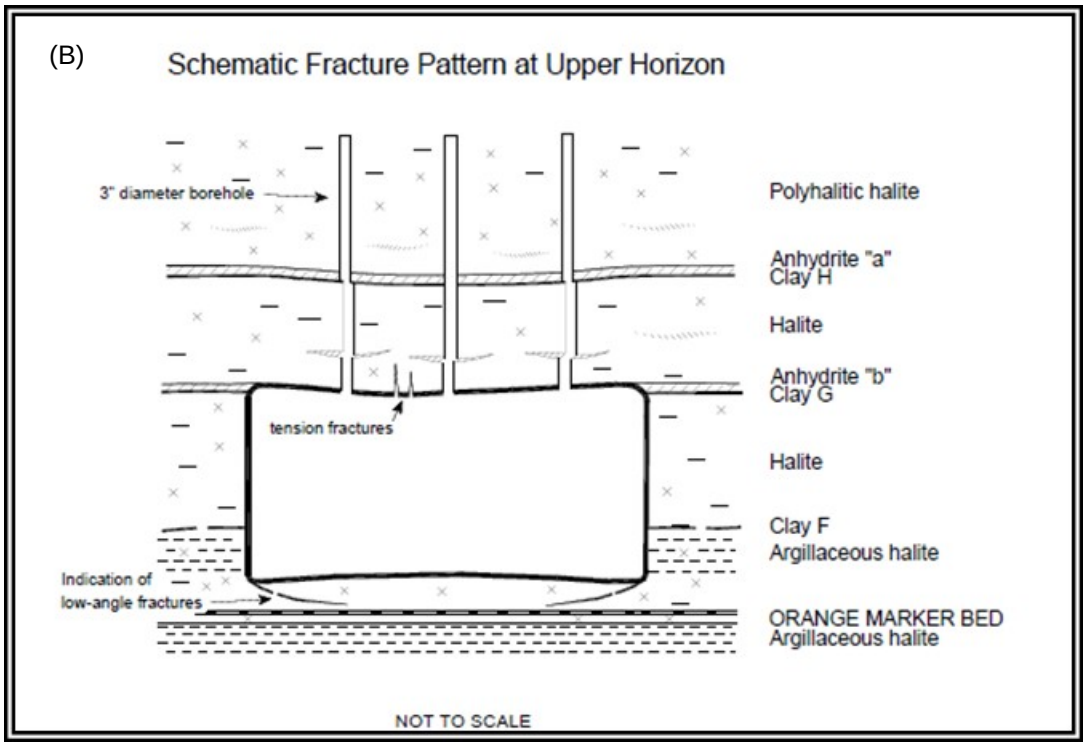

Figure 1. Typical rock failure modes around opening in the (A) lower horizon and (B) upper horizon (DOE/WIPP 2016).

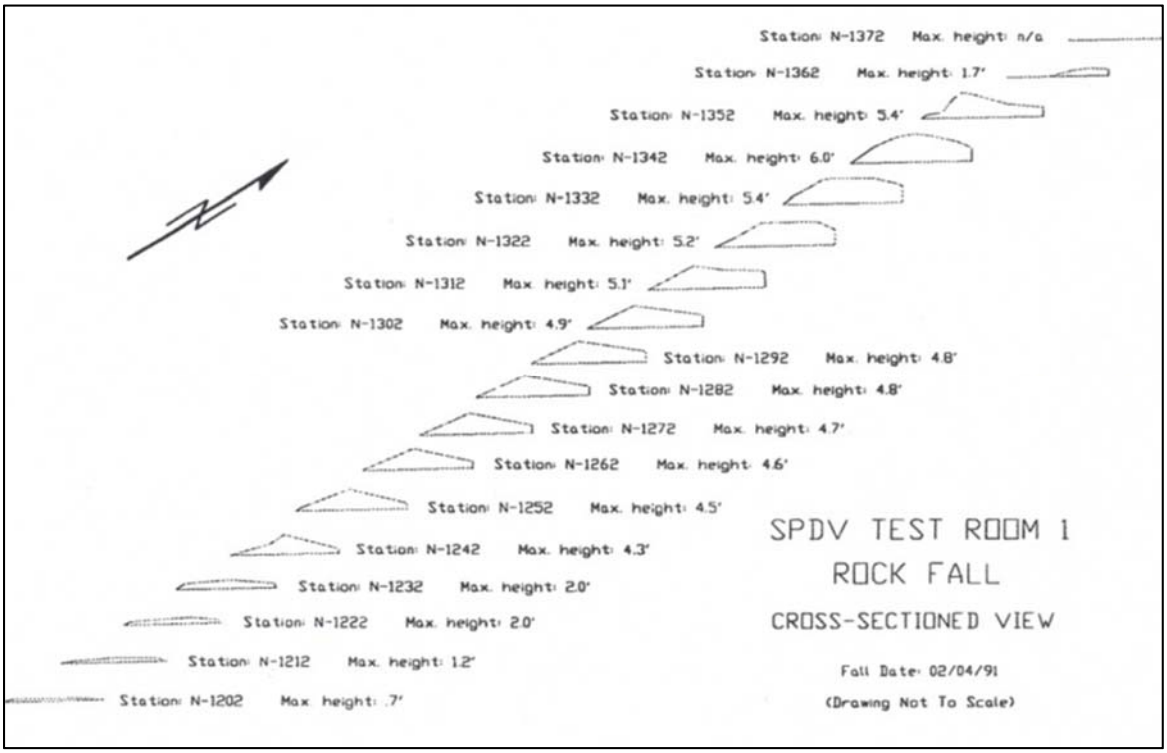

Figure 2. Cross-sectional shapes of the roof fall in SPDV Room 1 (DOE/WIPP 1993, Figure 3-1).

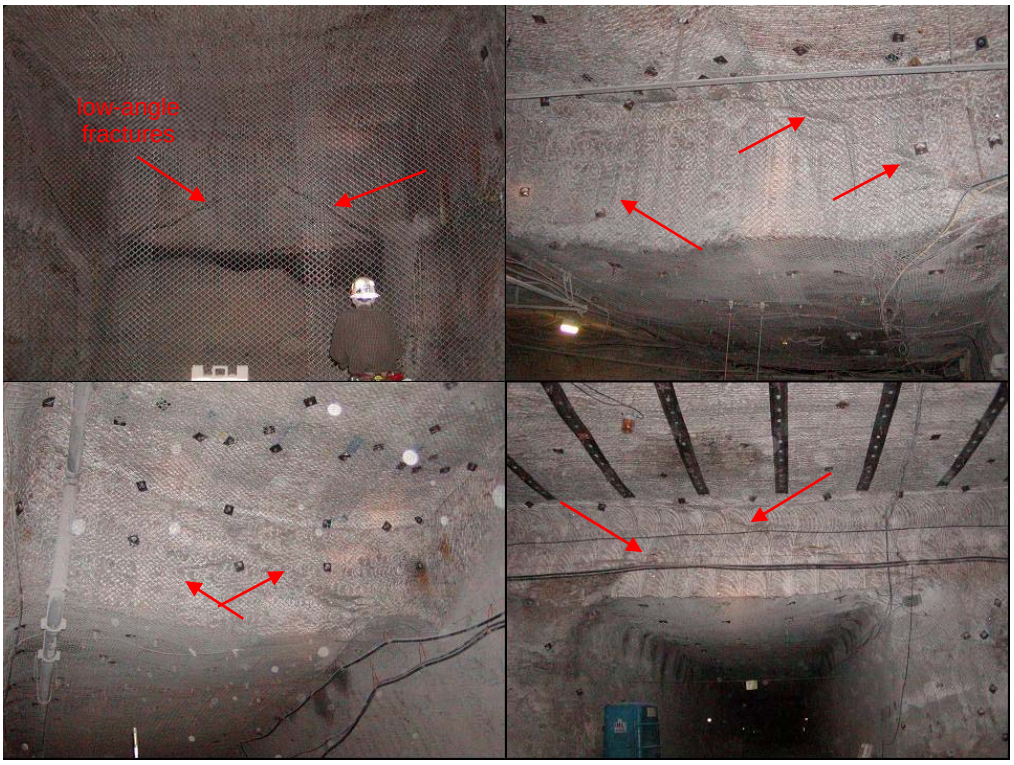

Figure 3. Photographs of rock fracturing around various WIPP underground openings. Failure modes correspond mostly with Figure 1A.

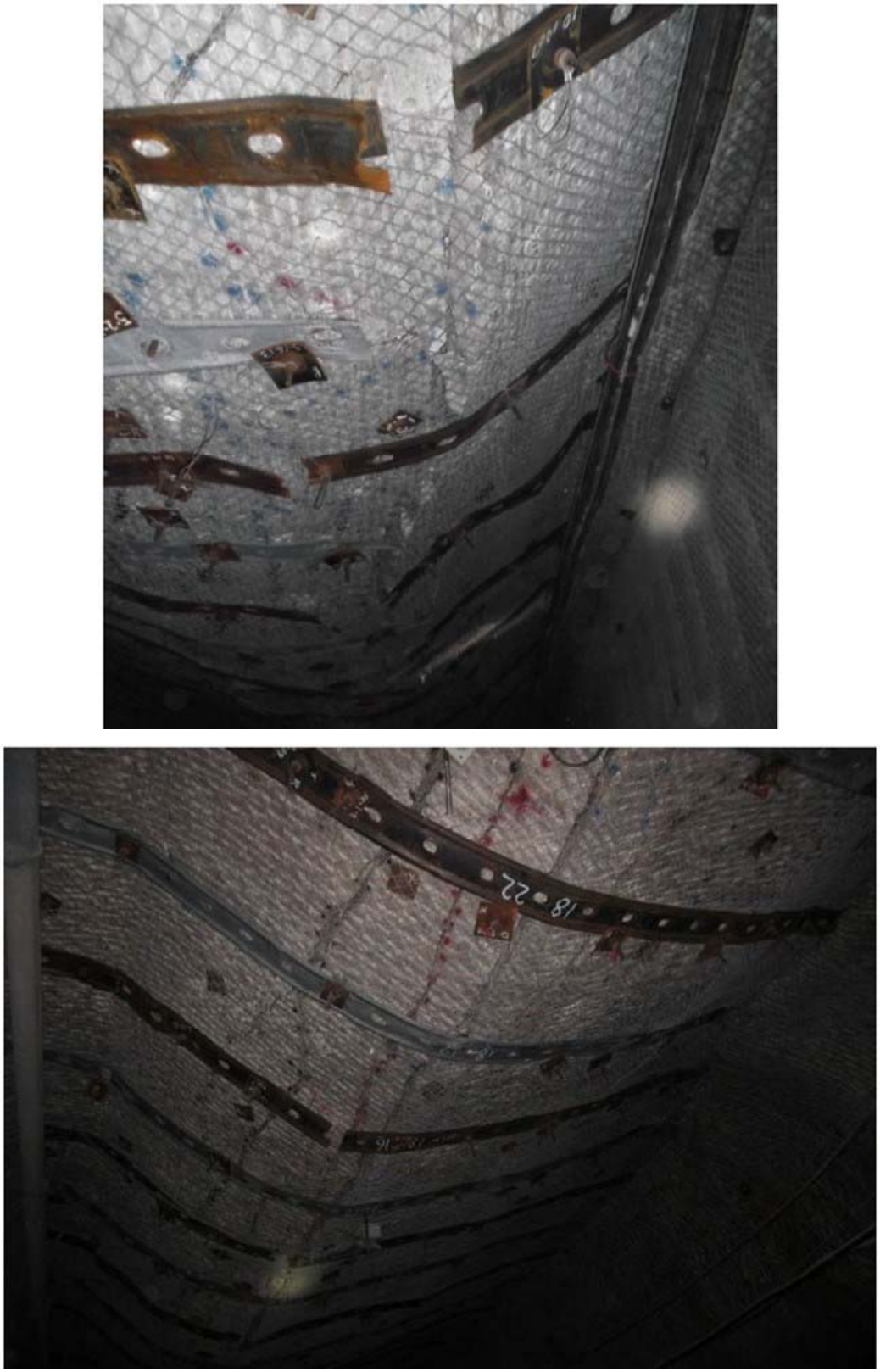

Figure 4. Photographs of the roof along E-140 drift.

Figure 5. Floor heave in Panel 7.

The decision to move to the upper horizon was made to avoid some of the ground control issues that were occurring in the lower horizon as noted above. It was felt that the ground control issues were less in the northern experimental area, which is at a higher horizon, and therefore raising the repository level would improve the ground control conditions.

In the upper horizon, the roof fractures differently (Figure 1B). Salt rock slabs separate from the rock above along anhydrite stringers (Figure 6). The slabs vary in thickness. As seen in Figure 6, the lower slab is approximately one foot in thickness; however, the slab above it is detached at the top of the room near Clay G and is several feet thick. To prevent the separation from becoming too large, NWP established a pattern bolting routine that was implemented within two weeks of mining a room. Another stringer, about a foot above the lower slab's separation plane, is visible as a thin light seam. No separation is visible on that stringer.

This produces a situation identical, but flipped vertically, to that shown in (Figure 5). Lateral compression causes the roof beams to buckle, increasing the separation distance.

Figure 6. Photograph of the brow of a room showing where separation has occurred along anhydrite stringers.

Boreholes in the ribs show systems of vertical, arcuate fractures that are concave towards the opening. Idealized cross-sections of rooms in WIPP are shown in Figure 7 (from Borns and Stormont 1988 and 1989) which depict the fractures in the ribs. Sonic velocity tests conducted by Holcomb and Hardy, as analyzed by Park et al. (2008) and Herrick et al. (2009), suggest that the fractures do not extend beyond the level of the corners of the roof and floor; however, the number of fractures and the depth into the rock at which they occur increases along the room's mid-height. The DRZ based on back-calculating the constant in a linear dilatant damage criterion (Van Sambeek et al. 1993) is shown in Figure 8. Time = 0.0 years assumes that this is the stress condition immediacy after excavation. Given that the corners of the room are stress concentrations, one might be surprised to see the lack of DRZ predicted there. The deviatoric stress is large at the corners, but the hydrostatic pressure is also large enough to inhibit fracturing.

Again, the accumulation of fractures in the ribs delineates relatively thin rock slabs. And in a manner similar to what occurs in the floor and roof, the compressive stress condition causes the pillars to bulge because of Poisson's effect and the slabs to buckle and bow inward. In extreme cases the walls may spall off.

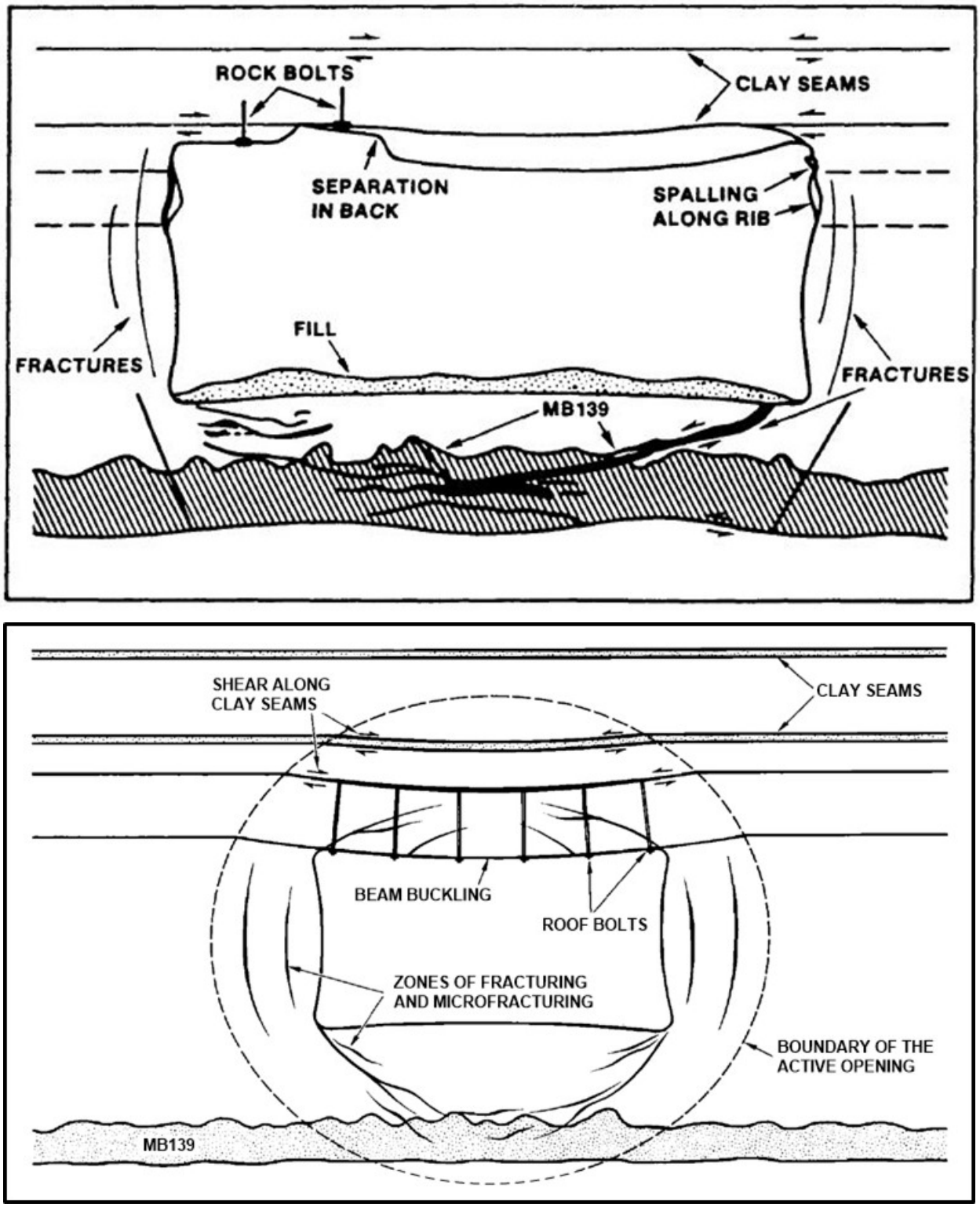

Figure 7. Idealized schematics of fracturing patterns around openings in the WIPP underground (Borns and Stormont 1988 and 1989).

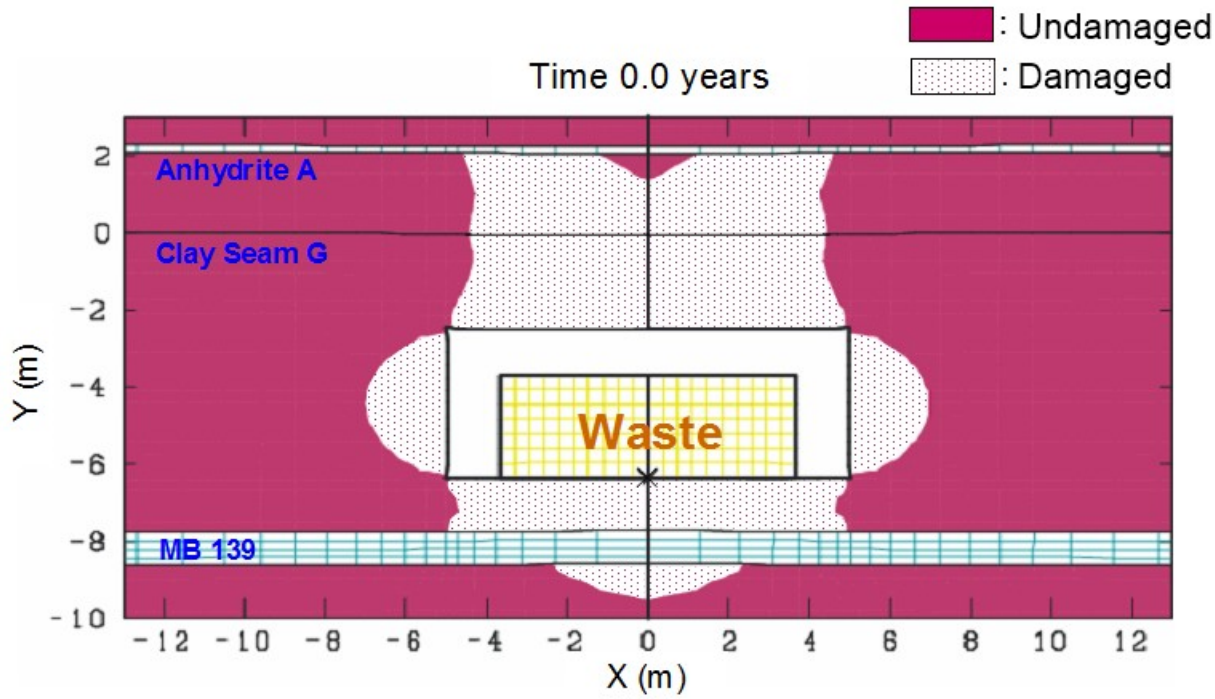

Figure 8. Maximum extent of the DRZ around a WIPP disposal room based on a site-specific dilatancy damage criterion (Herrick et al. 2009).

Room closure is the measured distance from one surface to the opposing surface. Generally, the middle of the room is most often referred to. These measurements are without a doubt influenced by the amount of bowing the rock slabs surrounding the opening have undergone. The longer the slabs, the more flexure they can undergo. The roof and the floor will create the longest detached slabs and therefore the greatest closure will occur between those two surfaces. The influence of fractures is magnified in cases such as E-140 where the blocks in the roof are detached. It is believed that closure measurements are capturing the flexure of the slabs and separation distances between of the fractures between slabs much more than they are reflecting creep of the rock salt. If it is indeed the case that room closure measurements are dominated by fracture growth and slab buckling, modeling this behavior with a continuum model of salt creep is problematic, especially in open, unfilled rooms where the supporting forces of the emplaced waste are not present to arrest closure. An appropriate model should allow for salt damage and/or fracture initiation and growth and may need to model discrete/discontinuous material behavior in both open and filled disposal rooms

3 Approach

The approach for re-evaluating the WIPP geomechanical model for room closure is to first assess discrepancies in current model predictions versus measured closure from Room D in the WIPP experimental area. The following open topics may be addressed:

- Creep behavior at low equivalent stresses
- Extent of the simulation area
- 1983 reference stratigraphy versus Munson 1989 stratigraphy
- Creep behavior of clean salt versus argillaceous salt
- Lost transient strains
- Sliding at clay seams
- Anhydrite strength

The next step is to assess the results from a set of laboratory tests that will be conducted to simulate actual openings underground (Herrick et al. 2017). Based on the assessment of discrepancies between model predictions and laboratory tests, a description of the WIPP conceptual geomechanical model for room closure will be developed considering both waste-filled and open rooms.

3.1 Assessment of Model Predictions of Room Closure

Reedlunn (2016) describes updating legacy Room D simulations to today's computational standards by rectifying several numerical issues. Subsequently, the constitutive model used in previous modeling studies was recalibrated two different ways against a suite of new laboratory creep experiments on salt. Simulations with the new, laboratory-based, calibrations under-predict Room D vertical closure by 3.1 times (Reedlunn 2016). The causes for the poor match between predictions and measurements are not immediately apparent. The issues that may be examined are described in this section.

3.1.1 Creep Behavior at Low Equivalent Stresses

The new Munson-Dawson (M-D) model calibrations significantly under predict creep at low equivalent stresses. As presented by Reedlunn (2016, Figures 3.7b and 3.8b), the steady-state strain rate and the transient strain limit exhibit bi-linear behavior, while new model calibrations (1A and 1B) only capture the behavior for equivalent stresses $\sigma \geq 8$ MPa. Increasing the creep at low equivalent stresses would increase the amount of room closure, and the equivalent stress contours developed by Reedlunn (2016, Figure 4.2) suggest that this would have a substantial impact on Room D predictions. While the strains are small, the vast majority of salt within 50 m of Room D has low equivalent stress. Integrating small strains over the simulation volume may add up to a significant displacement.

3.1.2 Extent of the Simulation Area

A question related to the creep at low equivalent stresses is, "How far away should the simulation boundaries be from the room?" According to Munson et al. (1986), "The right boundary distance (50 m) was chosen so that room response would not be affected by boundary conditions." A distance of 50 m may have been far enough during the initial simulations with the 1983 reference law, which significantly under-predicted Room D closure. However, 50 m does not appear to be far enough when the simulation nearly matches the closure measurements. The traction on the right boundary is plotted in Figure 9 for a clean salt simulation without any clay seams, and an all clean

salt simulation with sliding at the clay seams. Both simulations use the legacy clean salt calibration and are compared at time t =1,354 days. The traction distribution is non-linear, less than the lithostatic pressure, and quite erratic if the clay seams are included. If the right boundary was far enough away from the disturbance created by the void of Room D, then the traction distribution would be lithostatic. To the left of Room D, the distance to the nearest room (Room A3) is 85.3 m. This also is not far enough away to completely rule out interactions between the rooms. Future simulations should reassess how far away the top, bottom, left and right boundaries need to be such that increasing the distance further has no impact on the room closure.

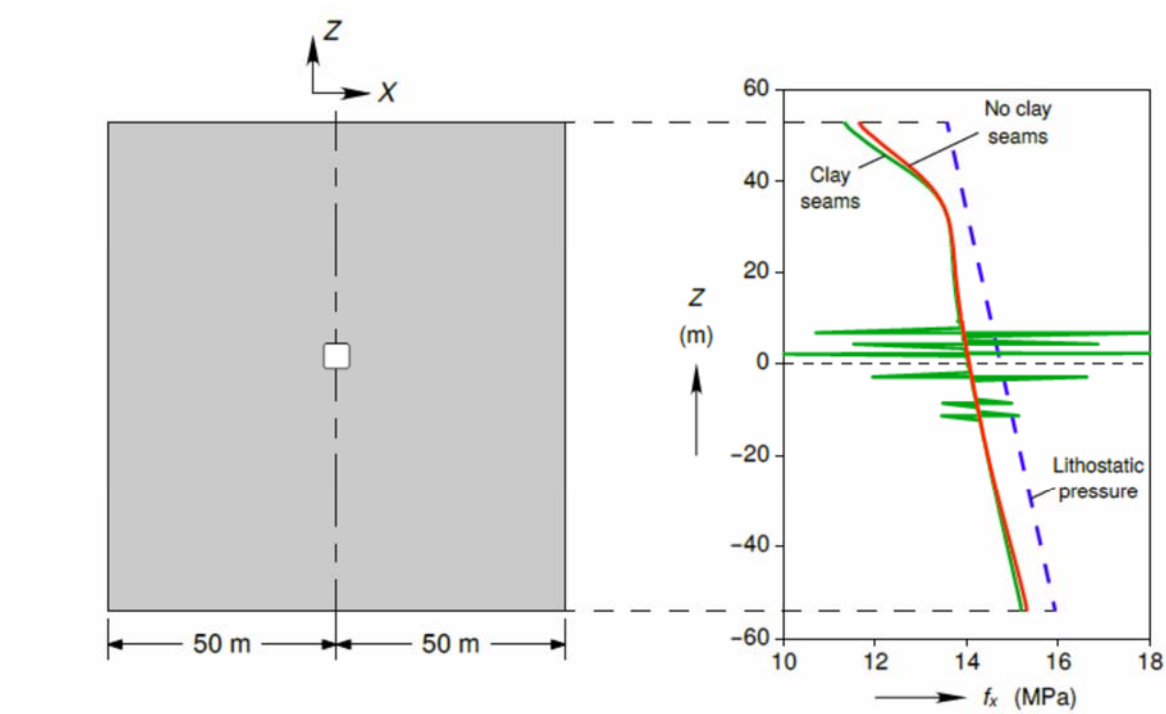

Figure 9. Horizontal traction (in the X-direction) along the right boundary of two all clean salt simulations at t = 1, 354 days. Both simulations used the legacy clean salt calibration (Reedlunn 2016, Figure 4.3).

3.1.3 1983 Reference Stratigraphy Versus Munson 1989 Stratigraphy

The 1983 reference stratigraphy was agreed upon by analysts, geologists, geophysicists, and mining engineers from the DOE, the Technical Support Contractor (D'Appolonia), and SNL. Munson et al. (1989) changed the idealized stratigraphy from mostly clean salt to mostly argillaceous salt, solely based on the visual appearance of cores drilled 15.2 m above and below Room D. Recently, Dennis Powers, a consulting geologist, was contracted by SNL to inspect cores from the Salt Disposal Investigations (SDI) area (Powers 2016). The cores (SDI-BH00004 and SDI-BH-00005) came from 15.5 m boreholes above and below the intersection of N780 and E1310. He concluded, "This study does not sustain the assessment of Munson et al. (1989) that all of the halite within the reference stratigraphy, with the exception of halite above and below anhydrite A, could or should be treated as argillaceous halite." He, on the other hand, stopped short of endorsing the 1983 reference stratigraphy, presumably because "[t]here appears to be sparse

data in which the weight % of clay can be compared to mechanical behavior." Without a correlation between non-halite components and mechanical behavior, it is difficult to decide where to draw the line between clean and argillaceous salt. Powers' evaluation of the stratigraphy data is expected to continue. In the end, the WIPP community needs to reach a consensus on an official stratigraphy for geomechanical modeling.

3.1.4 Creep Behavior of Clean Salt and Argillaceous Salt

Munson et al. (1989) chose to distinguish between clean and argillaceous salt based on the experiments in Senseny (1986). Similar differences between clean and argillaceous salt were later found in Mellegard and Pfeifle (1993). Despite scatter in the measurements, argillaceous salt creeps more than clean salt at all temperatures and stresses (Reedlunn 2016, Figure 4.4).

This result is inconsistent with the German measurements on the 2013 cores as part of Joint Project III, so the legacy and German measurements were directly compared by Reedlunn (2016, Figure 4.5). Considering adjustments for test temperature and differences in experimental procedure, the legacy and German measurements agree reasonably well for the clean salt, but not for the argillaceous salt (Reedlunn 2016, Figure 4.5). The argillaceous salt used in the legacy studies seems to creep more than the argillaceous salt used in the German measurements.

The root of the discrepancy between the legacy argillaceous salt and 2013 core argillaceous salt is unknown. The report by Senseny (1986) is perhaps the only study to measure the composition of clean and argillaceous WIPP salt specimens before creep testing. He found that, "[t]he average water and EDTA insoluble content of the argillaceous salt was 1.5 to 0.75%, respectively." Yet, "... the small amount of insolubles [in] the argillaceous specimens correspond to systematic increases in the creep deformation over that of clean specimens. The differences obtained are usually small, as less than an order of magnitude difference in the steady-state strain rate is generally observed. This result is in contrast to that obtained by Hansen et al. [1988b]. In their study using salt from the Palo Duro Basin, no influence of clay impurities on creep deformation was detected for impurity contents up to 25 percent."

Salt creep's sensitivity to moisture may be one potential reason for the difference between the Senseny (1986) and Hansen et al. (1988b) results. According to Senseny (1986), "[t]he argillaceous salt was sealed after drilling, but the clean salt was not." Once the cores arrived at RE/SPEC and the specimens were prepared, the "[a]rgillaceous specimens were immediately sealed by wrapping in aluminum foil and dipping in plastic coating. They remained sealed until they were jacketed for testing. Clean specimens were not sealed." Similar statements can be found in Mellegard and Pfeifle (1993). All of the 2013 cores, on the other hand, were treated the same way. They were packaged to avoid exposure to large volumes of air, and the creep specimens were drilled out of the larger 300 mm × 600 mm cores. Presuming the 2013 core preparation was equivalent to sealing, then one would expect the 2013 cores to creep similar to the legacy argillaceous cores. Reedlunn (2016, Figure 4.5), however, shows that the 2013 cores creep similar to the legacy clean cores. Thus, the selective sealing the legacy argillaceous cores does not fully explain the differences in behavior. To further complicate matters, the 2013 cores were drilled decades after the drifts were excavated. The constant flow of air through the drift may have desiccated the salt surrounding the drifts. Düsterloh et al. (2015) found the clean and argillaceous

salt contained roughly 0.15% and 0.35% water content, respectively, but moisture content was not measured on the legacy creep specimens, so a direct comparison is not possible.

Another potential reason for the increased creep in the legacy argillaceous salt cores is that cores from one location at WIPP may behave differently than cores from another location. Senseny (1986) and Mellegard and Pfeifle (1993) say the specimens were cored from the ribs of the experiment rooms at the WIPP. No further information is given, so the drill sites cannot be pinpointed as was done for the 2013 cores from Joint Project III.

This discussion underscores the need to (1) always document where cores came from at WIPP, (2) seal all specimens immediately after drilling, and (3) measure the composition and moisture content before mechanical testing. In the event that composition plays a role, it may be necessary to also investigate the spatial distribution of the impurities in the halite microstructure. Finely dispersed particles may impact the mechanical behavior very differently than large inclusions at the grain boundaries, for example.

3.1.5 Lost Transient Strains

All 2013 cores from Joint Project III were extracted from drifts, but Munson et al. (1989) trusted creep specimens that came from boreholes, such as ERDA-9, more than specimens that came from drifts for transient strain limit measurements. They argued that the salt surrounding a drift experiences a significant amount of transient strain after the drift is excavated. A specimen extracted from near that drift will have undergone a degree of deformation. Some of the transient strain is not accounted for and is often referred to as “lost” transient strain. For this reason, Munson et al. (1989) placed the transient strain limit at the upper edge of the clean salt experimental data (Reedlunn 2016, Figure 1.12c).

Two studies of dislocation density in salt crystals support the assertion that drift cores should not be considered virgin. Hansen (1988) compared the dislocation density of specimens extracted from the ribs of drifts at WIPP against that of ERDA-9 specimens at the Room D horizon. Dislocation density increases as salt work hardens, and Hansen (1988) found that the dislocation density of the drift specimens was two to three times higher than those of the ERDA-9 salt specimens. In a follow-up study, Hansen et al. (1988a) found, “dislocation density varies monotonically as a function of horizontal depth into the rib, ranging from 5.4 to 2.4×10^7 cm^2 between 0.3 and 14.3 m depth, respectively. Density of the laterally equivalent ERDA-9 salt is 1.7×10^7 cm^2.” The horizontal depth of the 2013 cores ranged from 0.7 m to 4.9 m (Reedlunn 2016, Section 3.1).

To quantify the amount of lost transient strain, Senseny (1990) performed three creep tests on ERDA-9 cores from the Room D horizon and three annealed drift core specimens. Senseny (1990) heated drift cores to 200ºC for 65 hours to anneal them. He compared his ERDA-9 results to existing results on drift core on a log transient strain vs. log stress plot, but he did not include his annealed drift core results, or results from ERDA-9 cores from other elevations. Reedlunn (2016) gives a more holistic picture, with solid markers for drift core specimens, and hollow markers for borehole core specimens or annealed drift core specimens (Figure 10).

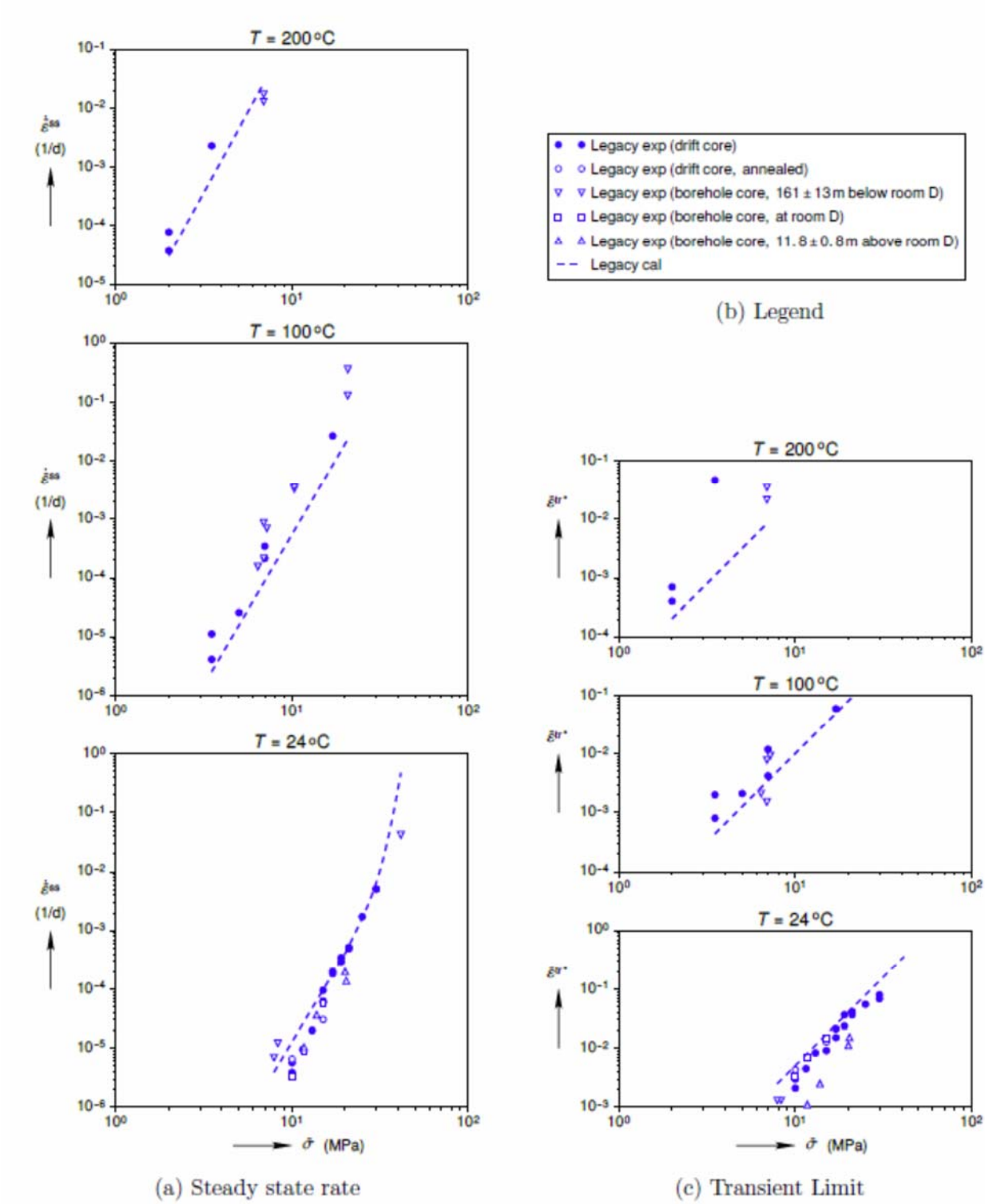

Figure 10. Legacy clean salt MD model calibration compared against clean salt creep measurements separated into various catagories (Reedlunn 2016, Figure 4.6).

A first glance at the values of transient strain limit in Figure 10c suggest that there might not be a systematic difference between drift cores and borehole cores. On the other hand, the approximate elevation of the borehole cores relative to Room D have been delineated, based on the specimen IDs and depths documented by Reedlunn (2016, Section 4.1.5). If one focuses on the drift cores and the borehole cores at Room D (ignore the triangle markers in Figure 10), the annealed cores and the borehole cores do have higher transient strain limit values than the drift cores at room temperature. Presumably, the borehole cores from other elevations (triangle markers) do not agree with the borehole and annealed cores from Room D due to creep property variations with respect to elevation. (This is probably why Munson et al. (1989) only used the transient strain limit measurements that came from cores at the elevation of Room D to select the transient stain limit constant K_0.) The annealed drift cores and the borehole cores at the elevation of Room D have roughly twice the transient strain of drift cores (Senseny 1990), which is not large on the log scale of Figure 10c. However, the comparison was done at medium to high equivalent stresses. The difference between borehole/annealed core and work hardened drift cores may become more significant at low equivalent stresses.

Creep tests on argillaceous borehole cores were not available in 1989, which is why Munson et al. (1989) felt justified placing the transient strain limit well above the argillaceous salt experimental data (Reedlunn 2016, Figure 1.12c). New tests on borehole cores have not been performed since 1989, but tests have been performed on argillaceous drift cores. Figure 11 compares the legacy argillaceous salt calibration against all the legacy argillaceous salt experiments. Notably, Mellegard and Pfeifle (1993) performed five room temperature tests on argillaceous salt specimens and two of them produced transient strain limit values that agree with the legacy argillaceous salt calibration. The room temperature plot in Figure 11b makes the argillaceous $K_0 = 2.470\times10^6$ value less speculative than the data that was available in 1989 (Reedlunn 2016, Figure 1.12c).

3.1.6 Sliding at Clay Seams

Morgan et al. (1986) found that reducing the coefficient of friction from $\eta = 0.4$ to 0 doubled the horizontal closure prediction of the south drift. This result is useful to get a sense of the sensitivity, but the clay seams are most likely not frictionless. Munson et al. (1989), in contrast, treated η as a free parameter and set it to 0.2. Reedlunn (2016) also used $\eta = 0.2$, except when the clay seams were eliminated to comply with the Joint Project III setup. If clay seams are not allowed to slide, the horizontal and vertical closures decrease by 19.4% and 27.0%, respectively, at time $t = 1{,}354$ days (Reedlunn 2016, Figure A.43a). Clearly, the clay seam behavior is too important to be simplified to Coulomb friction with η a free parameter. A laboratory program to test clay seams in direct shear could provide the data to develop a proper model for the seams (see Minkley and Mühlbauer 2007 for an example), and an underground in-situ test could help calibrate and/or validate such a model.

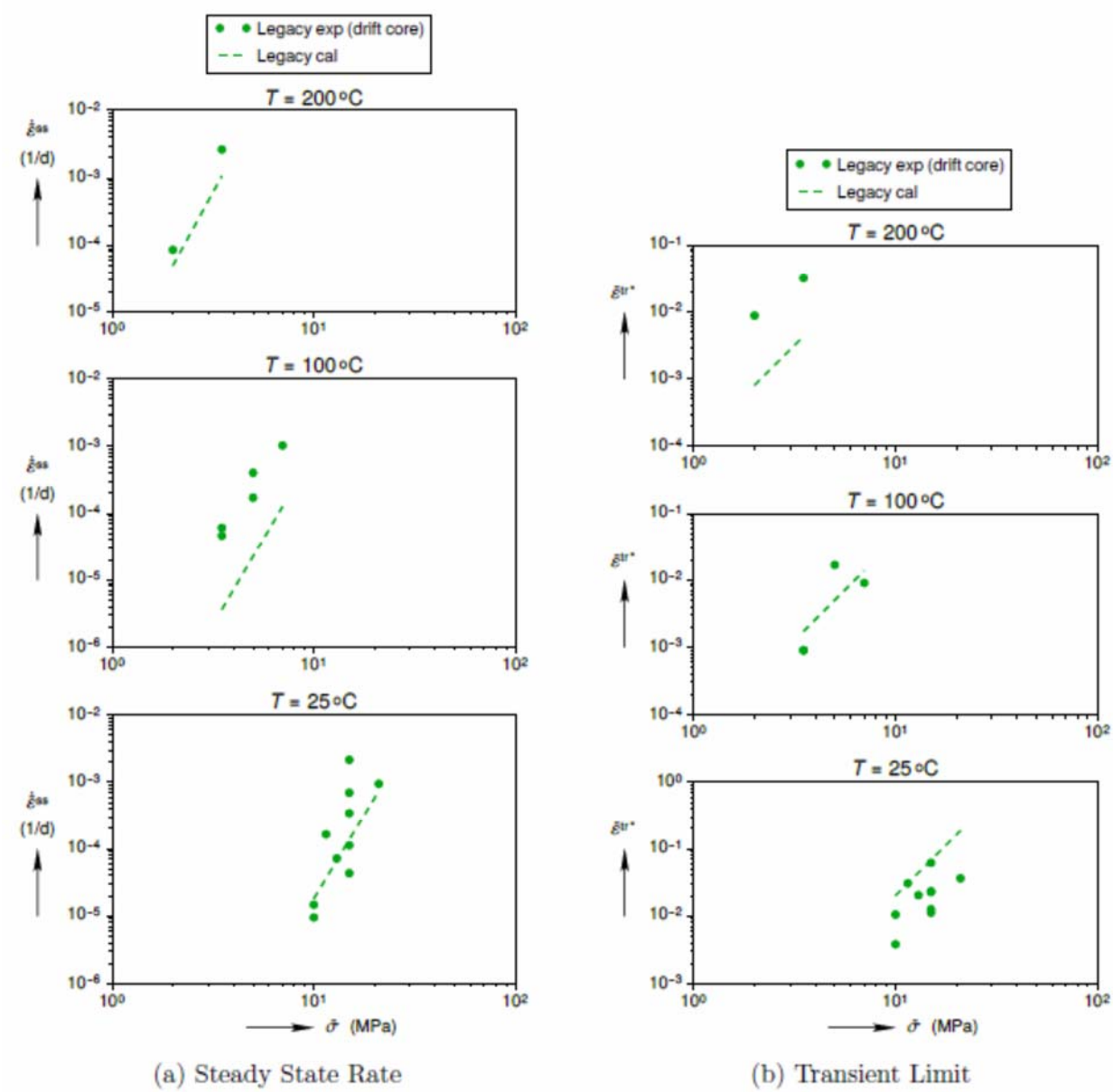

Figure 11. Legacy argillaceous salt MD model calibration compared against argillaceous salt creep measurements separated into various categories (Reedlunn 2016, Figure 4.7).

3.1.7 Anhydrite Strength

Similar to Argüello and Holland (2015) and Argüello (2015), Reedlunn (2016) found that including the anhydrite layers instead of treating them as salt decreased horizontal and vertical closures by about 20% at time t = 1,354 days. Morgan and Krieg (1984) selected the Drucker-Prager model parameters based on measurements of the yield and ultimate strength of anhydrite in Teufel (1981) and Senseny et al. (1983). The Joint Project III partners, however, selected a Mohr-Coulomb model with lower strengths. The Morgan and Krieg (1984) parameters, in their opinion, were too strong compared to values usually employed in the German salt community. In

a simulation without any clay seams, the weaker Mohr-Coulomb model increased the horizontal and vertical room closure by 15% and 19% compared to the legacy anhydrite model, at t = 1,354 days (Reedlunn 2016, Figure A.43a). Thus, the room closure is sensitive to the range of possible model parameters for the anhydrite model. A critical eye should assess the existing anhydrite calibration in Morgan and Krieg (1984) and any new experimental data in the literature. Analogous to the clay seams, a laboratory program may be necessary to characterize the anhydrite mechanical behavior properly.

3.2 Assessment of Laboratory Test Results

As described in Section 3.1, modeling efforts generally under-predict room closure with time by about a factor of three, which may in part be due to the model's inability to appropriately capture the impact of fracture development around underground openings. To investigate the impact of fracture development on room closure, a series of laboratory tests are proposed that simulate actual openings in the underground (Herrick et al. 2017). Specimens would be clean salt or salt including clay/anhydrite seams (Figure 12), with an opening drilled through the specimen. The tests should be run under both "predrilled" and "prestressed" conditions. A predrilled condition exists when the opening is drilled into the specimen prior to loading. A prestressed condition exists when the hole is drilled into the specimen after it is placed into the loading cell and the far-field stresses are applied. Predrilled tests are easier to perform and can be run under uniaxial, hydrostatic, triaxial, and true triaxial conditions. Prestressed tests require using an appropriate loading cell. The loading conditions could be hydrostatic, triaxial, and true triaxial. In addition, some tests will be performed for long periods of time. These tests provide time-dependent deformational behavior of salt determined through a series of triaxial compression constant stress creep tests (Herrick et al. 2017).

The tests, which are described by Herrick et al. (2017), seek to address the question: "when do the fractures form?" Do the fractures form immediately around the drilled opening when loaded, or does the salt's plasticity inhibit the formation of the fractures? WIPP field observations may indicate that the fractures form immediately around openings based on NWP's requirement to install pattern bolting within two weeks of excavation. The importance of these tests is to address the applicability of a continuum model for room closure versus the use of a discontinuous discrete fracture model.

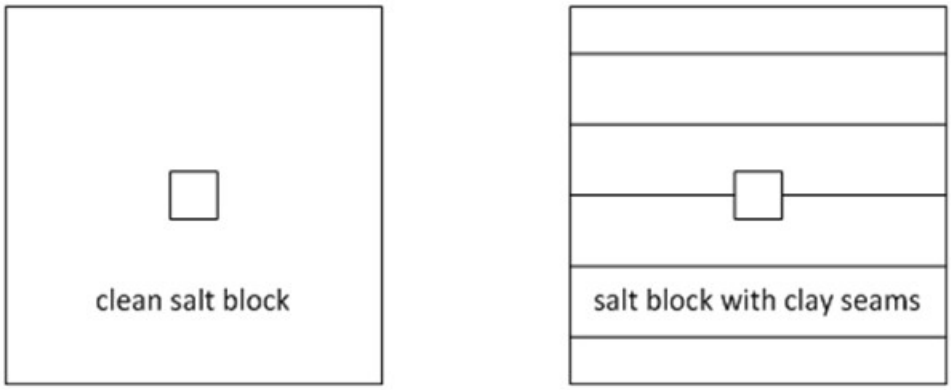

Figure 12. Idealized specimen geometries.

3.3 Numerical Modeling Techniques

Damage induced softening and fracturing are difficult processes to simulate in the finite element method. They cause pathological mesh dependence, where simulation results do not converge with mesh refinement. A host of numerical techniques have been developed to alleviate this issue over the last several decades. These techniques include non-local averaging of field variables, cohesive zone elements, the extended finite element method, particle based methods, and many others. Each approach has strengths and weaknesses in different applications. For example, non-local averaging of field variables is well suited to damage induced softening, but it may have trouble with macroscopic fractures.

A survey of these numerical modeling techniques will be conducted to assess which approach, if any, will meet the WIPP geomechanical modeling goals. Such a survey will include screening the available techniques, testing them on relatively simple boundary value problems, assessing whether the relevant physical behaviors are sufficiently mesh insensitive, and reporting the results.

3.4 Development of an Updated WIPP Conceptual Geomechanical Model for Room Closure

The current conceptual model for the geomechanical closure of excavated rooms at WIPP considers only creep closure – the gradual, continuous movement of salt from the formation into the void space of the rooms. The conceptual model focused on a disposal room that is waste-filled. Three processes were conceptualized during closure: (1) the volume of the excavation decreases with time as salt deforms to encapsulate the waste, (2) brine migrates from the formation toward the excavation because of the fluid pressure difference, and (3) decomposition, corrosion, and radiolysis processes within the waste generate gas (Butcher 1997, Section 2.1.3). Closure continues with time until the forces resulting from creep closure equilibrate with the backstress applied by the waste, brine, and gas.

In current PA modeling, both creep closure of the salt and the presence of either brine or gas in the WIPP waste disposal region influence time-dependent changes in void volume in the waste disposal area. As a consequence, these processes influence two-phase fluid flow of brine and gases through the disposal area and its capacity for storing fluids. For PA, a porosity surface method is used to indirectly couple mechanical closure with two-phase fluid flow calculations implemented in the BRAGFLO code. The porosity surface approach is used because current codes are not capable of fully coupling creep closure, waste consolidation, brine availability, and gas production and migration.

Creep closure is accounted for in BRAGFLO by changing the porosity of the waste disposal area according to a table of porosity values, termed the porosity surface. The porosity surface is generated using a nonlinear finite element code. Disposal room porosity is calculated over time, for different rates of gas generation and gas production potential, to construct a three-dimensional porosity surface representing changes in porosity as a function of pressure and time over the 10,000-year simulation period.

An updated WIPP conceptual geomechanical model for room closure will be developed that takes into consideration:

- Simulations of empty room closure — An abandoned panel with no waste emplaced will result in a large volume of open, unfilled drifts, that was not represented in the previous conceptual model for room closure.
- Discrete ground closure events — Recent observations of roof, rib, and floor instability and failure at WIPP suggests discrete room closure events should be considered together with creep closure.
- Field measurements of closure — An updated assessment of model predictions compared to field measurements of room closure will inform the development of conceptual geomechanical model.
- Laboratory test results — An updated assessment of laboratory testing that simulates actual openings underground will inform the development of conceptual geomechanical model.
- Identification of numerical modeling techniques — Given the considerations listed above, appropriate numerical techniques to model damage and failure behavior impacting room closure will be investigated.
- Field measurements of fracturing — Predictions of the DRZ and fractures around rooms at the WIPP will be compared against field observations and measurements.
- Salt reconsolidation — Modeling of the reconsolidation of salt blocks that have collapsed into open rooms will be investigated.
- PA modeling approach — Issues related to characterizing and modeling porosity and permeability due to creep, damage, fracturing, and reconsolidation will be investigated.

The updated conceptual geomechanical model will provide the approach for predicting the closure of open and filled rooms considering discrete events such as rock fall and floor heave coupled with creep closure mechanisms.

4 Reports and Documentation

One or more analysis reports will be generated as a result of this analysis plan. The analysis report(s) will present and discuss the following:

- Discrepancies in model predictions versus measured closure
- Comparisons between laboratory tests that simulate actual openings underground and model predictions
- Comparisons between field observations of DRZ/fractures and model predictions
- The approach for modeling room closure, including (1) the identification of appropriate numerical techniques to model damage and failure in both open and filled disposal rooms, (2) the consideration of salt reconsolidation, and (3) the identification of issues related

characterizing and modeling porosity and permeability due to creep, damage, fracturing, and reconsolidation.

5 Tasks

The tasks, responsible personnel, and estimated task schedule are summarized in Table 1. The completion date and responsible individuals may change in the future.

6 Software

Commercial off-the-shelf (COTS) software may be used in the development of the analysis report including, but not limited to Access®, Excel®, Grapher®, Kaleidagraph®, MATHEMATICA®, MATHCAD®, MATLAB®, or Python, running on workstations. The use of any COTS application will be documented and verified per Nuclear Waste Management Procedure NP 9-1, Section 2.2 as appropriate. Acquired software, including Sierra Mechanics, Dakota, and Cubit, may also be used in the development of the analysis report and will be qualified prior to use under NP 19-1.

7 Special Considerations

None

8 Applicable Procedures

All applicable WIPP QA procedures will be followed when conducting these analyses.

- Training of personnel will be conducted in accordance with the requirements of NP 2-1, *Qualification and Training*.
- FEPs assessment will be conducted according to SP 9-4, *Performing FEPs Impact Assessment for Planned or Unplanned Changes*.
- Analyses will be conducted and documented in accordance with the requirements of NP 9-1, *Analyses*.
- All software used will meet the requirements laid out in NP 19-1, *Software Requirements* and NP 9-1, as applicable.
- The analyses will be reviewed following NP 6-1, *Document Review Process*.
- All required records will be submitted to the WIPP Records Center in accordance with NP 17-1, *Records*.
- New and revised parameters may be created as discussed in NP 9-2, *Parameters.*

Table 1: Task list and estimated schedule for reconsideration of the WIPP geomechanical model for room closure

Task	Description	Guiding Document	Approximate Completion Date	Responsible Individual(s)
1	Analyze discrepancies between measured closure and model predictions without damage and fracture	AP-178	21 JUN 2018	Benjamin Reedlunn
2	Analyze results from laboratory tests that mimic underground openings	AP-178	19 JUL 2018	Courtney Herrick
3	Investigate numerical methods to model damage and fracture. Conduct initial simulations of laboratory tests that mimic underground openings.	AP-178	19 OCT 2018	Benjamin Reedlunn
4	Conduct initial simulations of the closure of a waste filled room and an empty room to demonstrate the new WIPP geomechanical model.	AP-178	19 OCT 2018	Dwayne Kicker and Benjamin Reedlunn
5	Document the results in an analysis report, "Reconsideration of the WIPP Geomechanical Model for Room Closure"	AP-178 NP 9-1	20 DEC 2018	Dwayne Kicker, Benjamin Reedlunn, and Courtney Herrick

9 References

Argüello, J.G. 2015. *Summary of FY15 Results of Benchmark Modeling Activities*. SAND2015-6273, Albuquerque, NM: Sandia National Laboratories.

Argüello, J.G. and J.F. Holland 2015. "Two Problems to Benchmark Numerical Codes for Use in Potential HLW Salt Repositories," *Proceedings of the Mechanical Behavior of Salt VIII*, pp. 361–371. London: Taylor & Francis Group.

Borns, D.J. and J.C. Stormont 1988. *An Interim Report on Excavation Effect Studies at the Waste Isolation Pilot Plant: The Delineation of the Disturbed Rock Zone*. SAND87-1375. Albuquerque, NM: Sandia National Laboratories.

Borns, D.J. and J.C. Stormont 1989. "Delineation of the Disturbed Rock Zone Surrounding Excavations in Salt," *Rock Mechanics as a Guide for Efficient Utilization of Natural Resources – Proceedings of the 30th U.S. Symposium on Rock Mechanics*, pp. 353-360. Rotterdam, Netherlands: Balkema.

Butcher, B.M. 1997. *Waste Isolation Pilot Plant Disposal Room Model*. SAND97-0794. Albuquerque, NM: Sandia National Laboratories.

DOE/WIPP 1993. *The Current Bases for Roof Fall Prediction at WIPP and a Preliminary Prediction for SPDV Room 2*. DOE/WIPP 93-033. Carlsbad, NM: U.S. Department of Energy, Carlsbad Field Office.

DOE/WIPP 2016. *Geotechnical Analysis Report for July 2014 – June 2015*. DOE/WIPP-16-3559, Volume 1. Oak Ridge, TN: U.S. Department of Energy, Office of Scientific and Technical Information.

Düsterloh, U., K. Herchen, K.-H. Lux, K. Salzer, R.-M. Günther, W. Minkley, A. Hampel, J.G. Argüello, and F. Hansen 2015. "Joint Project III on the Comparison of Constitutive Models for the Mechanical Behavior of Rock Salt: III. Extensive Laboratory Test Program with Argillaceous Salt from WIPP and Comparison of Test Results," *Proceedings of the Mechanical Behavior of Salt VIII*, pp. 13–21. London: Taylor & Francis Group.

Hansen, F.D. 1988. Memorandum to D.E. Munson Re: Substructures of Undeformed WIPP and ERDA-9 Salt, February 19, 1988. ERMS 305251.

Hansen, F.D., D.E. Munson, and A.F. Fossum 1988a. "Substructures of Salt from the WIPP Site," Poster, American Geophysical Union Fall Conference.

Hansen, F.D., P.E. Senseny, T.W. Pfeifle, and T.J. Vogt 1988b. "Influence of Impurities on the Creep of Salt from the Palo Duro Basin," *Proceedings of the 29th US Symposium on Rock Mechanics*. American Rock Mechanics Association.

Herrick, C.G., B.Y. Park, M.Y. Lee, and D.J. Holcomb 2009. "Estimating the Extent of the Disturbed Rock Zone around a WIPP Disposal Room," *Proceedings of the 43rd U.S. Rock Mechanics Symposium and 4th U.S.-Canada Rock Mechanics Symposium*, pp. 300-308. Alexandria, VA: American Rock Mechanics Association.

Herrick, C.G., B. Reedlunn, and R.P. Jensen 2017. *Experimental Investigation of Small-Scale Openings in WIPP Salt*. Test Plan TP 17-02. Carlsbad, NM: Sandia National Laboratories. ERMS 568416.

Mellegard, K.D. and T.W. Pfeifle 1993. *Creep Tests on Clean and Argillaceous Salt from the Waste Isolation Pilot Plant*. SAND92-7291. Albuquerque, NM: Sandia National Laboratories.

Minkley, W. and J. Mühlbauer 2007. "Constitutive Models to Describe the Mechanical Behavior of Salt Rocks and the Imbedded Weakness Planes," *Proceedings of the 6th Conference on the Mechanical Behavior of Salt – SALTMECH6*, pp. 22–25. London: Taylor & Francis.

Morgan, H.S. and R.D. Krieg 1984. Memorandum to D.E. Munson Re: Updated Drucker-Prager Constants for Anhydrite and Polyhalite. June 19, 1984. ERMS 542541.

Morgan, H.S., C.M. Stone, and R.D. Krieg 1986. *An Evaluation of WIPP Structural Modeling Capabilities Based on Comparisons with South Drift Data*. SAND85-0323. Albuquerque, NM: Sandia National Laboratories.

Munson, D. E., T. Torres, and D. Blankenship 1986. "Early Results from the Thermal/Structural In Situ Test Series at the WIPP," *Proceedings of the 27th US Symposium on Rock Mechanics*. Littleton, CO: Society of Mining Engineers.

Munson, D. E., A. F. Fossum, and P. E. Senseny 1989. *Advances in Resolution of Discrepancies Between Predicted and Measured In Situ WIPP Room Closures*. SAND88-2948. Albuquerque, NM: Sandia National Laboratories.

Park, B. Y., A.E. Ismail, D.J. Holcomb, and C.G. Herrick 2008. *Analysis Report for Prediction of the Extent and Permeability of the Disturbed Rock Zone around a WIPP Disposal Room*. Carlsbad, NM: Sandia National Laboratories. ERMS 546370.

Powers, D. 2016. Reference Stratigraphy Applied to Rock Mechanics Studies for the Waste Isolation Pilot Plant: A Review. Personal Communication, May 2016.

Reedlunn, B. 2016. *Reinvestigation into Closure Predictions of Room D at the Waste Isolation Pilot Plant*. SAND2016-9961. Albuquerque, NM: Sandia National Laboratories.

Senseny, P. E., A.F. Fossum, and T.W. Pfeifle 1983. "Non-associative Constitutive Laws for Low Porosity Rocks," *International Journal for Numerical and Analytical Methods in Geomechanics*, 7(1), 101–115.

Senseny, P.E. 1986. *Triaxial Compression Creep Tests on Salt from the Waste Isolation Pilot Plant*. SAND85-7261. Albuquerque, NM: Sandia National Laboratories.

Senseny, P.E. 1990. *Creep of Salt from the ERDA-9 Borehole and the WIPP Workings*. SAND89-7098. Albuquerque, NM: Sandia National Laboratories.

Teufel, L.W. 1981. *Mechanical Properties of Anhydrite and Polyhalite in Quasi-static Triaxial Compression*. SAND81-0858. Albuquerque, NM: Sandia National Laboratories.

Van Sambeek, L.L., J.L. Ratigan, and F.D. Hansen 1993. "Dilatancy of Rock Salt in Laboratory Tests," *International Journal of Rock Mechanics and Mining Sciences & Geomechanics Abstracts*, 30: 735– 738.

This work of authorship was prepared as an account of work sponsored by an agency of the United States Government. Accordingly, the United States Government retains a nonexclusive, royalty-free license to publish or reproduce the published form of this contribution, or allow others to do so for United States Government purposes. Neither the National Technology and Engineering Solutions of Sandia, LLC., the United States Government, nor any agency thereof, nor any of their employees makes any warranty, express or implied, or assumes any legal liability or responsibility for the accuracy, completeness, or usefulness of any information, apparatus, product, or process disclosed, or represents that its use would not infringe privately-owned rights. Reference herein to any specific commercial product, process, or service by trade name, trademark, manufacturer, or otherwise does not necessarily constitute or imply its endorsement, recommendation, or favoring by the National Technology and Engineering Solutions of Sandia, LLC., the United States Government, or any agency thereof. The views and opinions expressed herein do not necessarily state or reflect those of the National Technology and Engineering Solutions of Sandia, LLC., the United States Government or any agency thereof.

Sandia National Laboratories is a multimission laboratory managed and operated by National Technology and Engineering Solutions of Sandia, LLC., a wholly owned subsidiary of Honeywell International, Inc., for the U.S. Department of Energy’s National Nuclear Security Administration under contract DE-NA-0003525.

Parties are allowed to download copies at no cost for internal use within your organization only provided that any copies made are true and accurate. Copies must include a statement acknowledging Sandia's authorship of the subject matter.